JOURNAL OF PROPULSION AND POWER
Vol. 21, No. 4, July–August 2005

Swirling Inflow Within the Narrow Gap of Two Disks

G. H. Vatistas* and W. Ghaly†
Concordia University, Montreal, Quebec H3G 1M8, Canada
and
P. Tsifourdaris‡
Pratt and Whitney Canada Longueuil, Quebec J4G 1A1, Canada

The results of an analytical study dealing with the asymptotic swirling inflow, generated within the gap of two closely placed parallel disks, are presented. It is shown that the radial velocity component can be expressed by a single parameter, which combines the reduced Reynolds number and radial position. The latter velocity is found to flatten at the midgap position with the Reynolds number producing a plateau that progressively expands toward the walls. Under the action of viscous diffusion, the axial distribution of the tangential velocity is found to exhibit a similar property. The radial profile of the static pressure is shown to depend on the relative vortex strength and the Reynolds number. As inertia begins to dominate the viscous forces, the mid-channel tangential velocity curvature in the axial direction is found to tend asymptotically to zero, thus, encouraging the centerline velocity to approach the free-vortex profile. The results of the analytical study compare favorably with previous and present experimental evidence.

Nomenclature

A, B	=	arbitrary constants
h	=	half gap size, m
m, n	=	dummy variable
p	=	static pressure, Pa
R_e	=	exit radius, m
R_{in}	=	disk radius, m
Re	=	Reynolds number, $v_{r\mathrm{in}} h/\nu$,
Re_r	=	reduced Reynolds number, $Re\,\sigma$
r, θ, z	=	polar coordinates, m, rads, m
S	=	swirl ratio, $v_{\theta\mathrm{in}}/v_{r\mathrm{in}}$
$\mathcal{U}$	=	dimensionless radial velocity
V	=	dimensionless tangential velocity
v	=	velocity component, m/s
x, y, z	=	Cartesian coordinates, m
β_n	=	eigenvalues
Δp	=	dimensionless static pressure, $[p(r) - P_{\mathrm{in}}]\,/\,\rho v_{r\mathrm{in}}^2$
$\Delta\Pi$	=	dimensionless static pressure, $2\eta^2(\eta^2 - 1)\Delta p$
ζ	=	dimensionless axial coordinate
η	=	dimensionless radial coordinate
λ	=	dimensionless parameter
ν	=	kinematic viscosity, m^2/s
Ξ	=	general dimensionless pressure function
ρ	=	density, kg/m^3
σ	=	aspect ratio, h/R_{in}
Φ	=	general dimensionless velocity function
ω	=	rotational speed of the disks, rads/s

Subscripts and Superscript

in	=	properties at the inlet
max	=	maximum value of the quantity
r, θ, z	=	radial, tangential, and axial component
$*$	=	dimensional quantity

Received 6 March 2003; accepted for publication 29 January 2005.

*Professor, Mechanical and Industrial Engineering Department. Senior Member AIAA.

†Associate Professor, Mechanical and Industrial Engineering Department. Senior Member AIAA.

‡Senior Aerodynamicist, Turbine Aerodynamics.

I. Introduction

A VARIETY of fundamentally distinct flows are possible to evolve within the space formed by placing two flat disks one on top of the other (Fig. 1). Allowing the fluid to enter the gap by the periphery and to exit the domain from a centrally located outlet generates the accelerating (or sink) flow. This kind of fluid motion is characterized by a monotonically decreasing pressure gradient. The stabilizing effects of acceleration encourage the flow to remain laminar even at very high inlet Reynolds numbers, or to laminarize in the case that the entering flow is turbulent. A decelerating (or source) flow unfolds by reversing the flow direction of the previous case. Three particular flow manifestations are associated with the latter fluid motion. At relatively low inlet Reynolds numbers, a laminar flow throughout the gap emerges. In the case of intermediate inlet Reynolds numbers, a decaying, self-controlled oscillatory flow ensues. Finally, for high inlet Reynolds numbers, this condition is succeeded by a self-sustained fluctuating flow that matures into a laminar–turbulent transition, followed by a reverse flow transformation to laminarlike conditions at larger radii. Because the flow undergoes a continual variation of its velocity, the Stokesian flow assumption is not valid, even for low inlet Reynolds numbers. The complexity of the entire affair is exacerbated by the introduction of a centrifugal force field via either the imposition of swirl at the inlet, or the rotation of one or of both disks.

Flowfields of this kind are worth studying because these are routinely encountered in a number of standard technological applications such as radial diffusers, flow regulating valves, multiple-disk turbomachinery, air bearings, disk-type heat exchangers, pneumatic micrometers, flow and viscosity meters, vortex gyroscopes, and in a more exotic device such as the gaseous core nuclear rocket for advanced space propulsion. The industrial value of these types of flows is, therefore, evident. In addition, the topic is of academic interest. These are the incentives that have made the study of these flows attractive to both applied and theoretical fluid dynamicists for at least 50 years.

During this period, several papers related to the subject matter have been published that are too numerous to mention here. The earlier experiments of Morgan and Saunders[1] without swirl suggested that the inertia contribution could not be neglected, even at the viscous-dominated regime. Under this constraint, the momentum equation is nonlinear, and as a result only approximate solutions have been reported in the past. Many investigators presented solutions based on von Kármán's integral approach. Among those are Woolard,[2] Livesey,[3] Moller,[4] Boyack and Rice,[5] and Kwok and Lee.[6] A satisfactory solution for the pressure was obtained by

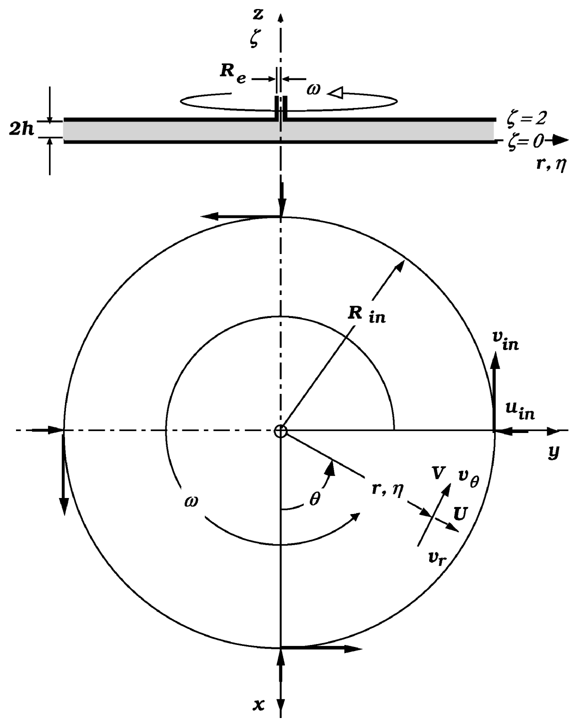

Fig. 1 Schematic of the problem.

Savage,[7] in the range of Moller's[4] experiments, by perturbing the parabolic velocity for the outflow case in terms of the downstream coordinate. Lee and Lin[8] obtained a solution to the linearized differential form of the momentum equation employing the Runge–Kutta numerical technique. Their static pressure results compared favorably with the experiments of Hayes and Tucker.[9] A further simplification of the inertial term led Vatistas[10] to a simple closed-form solution for the pressure. However, a radial velocity distribution of a creeping flow was assumed. In a subsequent paper by Vatistas,[11] an explicit solution to the equation of Lee and Lin[8] was reported. Numerical solutions to the inflow problem were presented by Murphy et al.[12] and by Zitouni and Vatistas.[13]

In the last 37 years, several papers related to disk flows with swirl have been reported. Although one can find earlier contributions, by a number of investigators, dealing with the heat transfer properties in domains similar to the one considered here, we will restrict our short review to contributions that deal strictly with isothermal flows. The experiments of Savino and Keshock[14] dealt with the experimental determination of velocity and pressure of a sink flow produced in a short cylindrical vortex chamber. Conover[15] studied experimentally the laminar flow developed between a rotating disk and a stationary wall with and without radial flow. DeSantis and Rakowsky[16] investigated the boundary-layer characteristics of the inward fluid motion in a pair of coaxial disks with weak swirl at the inlet. The turbulent source field between two corotating disks was the theme of the experimental and theoretical studies of Bakke et al.[17]

The present paper focuses on asymptotic solutions to the steady, laminar swirling sink flow between two flat disks where all material elements are monotonically accelerating in the radial direction. In other words, we are interested in the types of flow where the streamlines converge over the entire channel. There is at least one extreme value of the tangential velocity inside the gap, and the flow is symmetric about the midchannel plane. In the absence of swirl this problem is in many respects similar to Jefrey-Hamel flow within two inclined planes. Although the spacing between the two disks, in the present problem, remains constant, the flowfield experiences a similar effect because the perimeter of the area normal to the fluid motion changes with the radius. The main goal of the paper is to provide approximate expressions for the static pressure and the velocity.

II. Theoretical Development of the Problem

In this section, we focus on the analytical development of sink flows where the material elements are accelerating in the negative radial direction. The idealized problem is diagramed in Fig. 1. Fluid enters the domain from the periphery, and it exits through the centrally located outlet. Under the assumption that the flowfield is steady, laminar, incompressible, and axisymmetric, that the gap between the disks is very small ($h/R_{in} \ll 1$), and that $R_e \ll R_{in}$, the conservation equations in dimensionless form are as follows.

Continuity:

$$\frac{1}{\eta}\frac{\partial}{\partial\eta}[\mathcal{U}\eta] = 0 \tag{1}$$

The η momentum:

$$\mathcal{U}\frac{\partial\mathcal{U}}{\partial\eta} - S^2\frac{V^2}{\eta} = -\frac{d\Delta P}{d\eta} + \frac{1}{Re_r}\frac{\partial^2\mathcal{U}}{\partial\zeta^2} \tag{2}$$

The θ momentum:

$$\mathcal{U}\frac{\partial[V\eta]}{\partial\eta} = \frac{1}{Re_r}\frac{\partial^2[V\eta]}{\partial\zeta^2} \tag{3}$$

where all of the parameters are defined in the Nomenclature.

Equation (1) suggests that

$$\mathcal{U} = \Phi(\zeta)/\eta \tag{4}$$

This is, of course, the case if one stays away from the exit port where the fluid has not yet detected the outlet and the zero axial velocity assumption is asymptotically a valid hypothesis. When Eq. (4), is used, the inertial term ($\mathcal{U} \approx -1/\eta$) is linearized, and furthermore the centerline value for the tangential velocity ($V \approx V_{max}$) is taken to represent the centrifugal effects, the η-momentum equation simplifies to

$$-\frac{\Phi(\zeta)}{\eta^3} - \frac{S^2V_{max}^2}{\eta} = -\frac{d\Delta p(\eta)}{d\eta} + \frac{1}{Re_r\eta}\frac{d^2\Phi(\zeta)}{d\zeta^2}$$

Integrating the preceding equation with respect to η, from $\eta = 1$ to η, and noting that V_{max} is a function of η alone, we obtain

$$\frac{d^2\Phi(\zeta)}{d\zeta^2} - \frac{(\eta^2-1)Re_r}{2\eta^2\ln(\eta)}\Phi(\zeta) = \lambda^2\Delta\Xi(\eta) \tag{5}$$

where

$$\lambda = \sqrt{\frac{(\eta^2-1)Re_r}{2\eta^2\ln(\eta)}}, \qquad \Delta\Pi(\eta) = \Delta p(\eta)\frac{2\eta^2}{(\eta^2-1)}$$

Solution of Eq. (5) followed by the incorporation of the boundary nonslip condition for the radial velocity component in the ζ direction at $\zeta = 0$ and 2 yields

$$\Phi(\zeta) = \Delta\Xi(\lambda)\left\{\frac{\sinh[\lambda(2-\zeta)] + \sinh[\lambda\zeta]}{\sinh[2\lambda]} - 1\right\} \tag{6}$$

From the continuity constraint

$$\int_0^1 \Phi(\zeta)\,d\zeta = -1 \tag{7}$$

and Eq. (6), we have

$$\Delta\Xi(\lambda) = \frac{\lambda\sinh[2\lambda]}{\lambda\sinh[2\lambda] - \cosh[2\lambda] + 1} \tag{8}$$

Incorporation of the last result into Eq. (6) yields

$$\Phi(\zeta) = \frac{\lambda \sinh[2\lambda]}{\lambda \sinh[2\lambda] - \cosh[2\lambda] + 1} \times \left\{ \frac{\sinh[\lambda(2-\zeta)] + \sinh[\lambda\zeta]}{\sinh[2\lambda]} - 1 \right\} \tag{9}$$

Therefore, the dimensionless pressure is

$$\Delta\Pi(\eta) = \Delta\Xi(\eta) + S^2 \frac{2\eta^2}{\eta^2 - 1} \int_1^\eta \frac{V_{\max}^2}{\eta} \, d\eta \tag{10}$$

A. Swirl at the Inlet with Plates Stationary

To determine $\Delta\Pi$ and Φ, we have to derive an expression of $V_{\max}$. Linearization of the inertial term ($u \approx -1/\eta$) in Eq. (4) gives

$$-\frac{1}{\eta}\frac{\partial[V\eta]}{\partial\eta} = \frac{1}{Re_r}\frac{\partial^2[V\eta]}{\partial\zeta^2} \tag{11}$$

Partial differential equation (11) is solved by the standard separation of variables method. Applying the nonslip boundary condition for the tangential velocity component at $\zeta = 0$ and 2 and the entrance condition $\eta = 1 \rightarrow V = 1$, we obtain

$$V = \frac{2}{\eta}\sum_{n=0}^{\infty} \frac{\sin[\delta_n \zeta]}{\delta_n} \exp\left[-\frac{\beta_n^2}{2}(1-\eta^2)\right] \tag{12}$$

where

$$\beta_n = \left[(2n+1)\big/2\sqrt{Re_r}\right]\pi, \qquad \delta_n = [(2n+1)/2]\,\pi$$

$$n = 0, 1, 2, 3, 4, \ldots,$$

Because the maximum occurs at $\zeta = 1$, we have

$$V_{\max} = \frac{2}{\eta}\sum_{n=0}^{\infty} \frac{(-1)^n}{\delta_n} \exp\left[-\frac{\beta_n^2}{2}(1-\eta^2)\right] \tag{13}$$

The pressure can now be determined by inserting the expression for the maximum tangential velocity given by Eq. (13) into Eq. (10). The integral in Eq. (10) can be solved exactly. However, it will require the evaluation of double infinite series. A very accurate value can also be obtained by any standard integral numerical technique.

B. Swirl at the Inlet with Rotating Plates

The case where both disks are rotating and the fluid is entering the gap with an initial swirl requires special treatment. To make the boundary conditions homogeneous, the following transformation is utilized

$$\hat{V} = V + (Re_r/\eta)(\zeta^2 - 2\zeta) + \eta$$

Following a procedure similar to the preceding case, the tangential velocity component and the static pressure are given by

$$V = -\frac{4Re_r}{\eta}\sum_{n=0}^{\infty} \frac{\sin[\delta_n\zeta]}{\delta_n^3} \exp\left[-\frac{\beta_n^2}{2}(1-\eta^2)\right] + \frac{Re_r}{\eta}(\zeta^2 - 2\zeta) + \eta \tag{14}$$

where

$$V_{\max} = -\frac{4Re_r}{\eta}\sum_{n=0}^{\infty} \frac{(-1)^n}{\delta_n^3} \exp\left[-\frac{\beta_n^2}{2}(1-\eta^2)\right] + \frac{Re_r}{\eta} + \eta \tag{15}$$

The dimensionless static pressure distribution is also given by Eq. (10). Of course, the maximum tangential velocity distribution given by Eq. (15) must be used here.

III. Analysis of the Problem

The experimental data to be reported have been obtained using the apparatus shown in Fig. 2. It consists of two 0.457-m- (18-in.-) diam Plexiglas disks held stationary over a fixed support. The inflow is generated connecting the 0.032-m- (1.25-in.-) diam central outlet tube to the suction side of the compressor. Swirl is imparted into the entering fluid by fixing a swirl generator ring in the gap at the periphery having 50 tangential holes. The volumetric flow rate is metered by a rotameter. The radial static pressure distribution is picked up from nine equally spaced pressure taps located on the top plate and then measured by an inclined manometer.

It is evident from Eq. (9) that the radial velocity distribution is solely a function of parameter λ (or Reynolds number Re_r and η), and it is the same for both the earlier given cases. It is also similar to the nonswirling radial inflow, which indicates that under the mentioned assumptions the velocity component retains its general form. In Fig. 3, a family of velocity distributions is presented. For small values of Reynolds number Re_r the familiar Poiseuille-like profile similar to the flow between two flat plates is present.

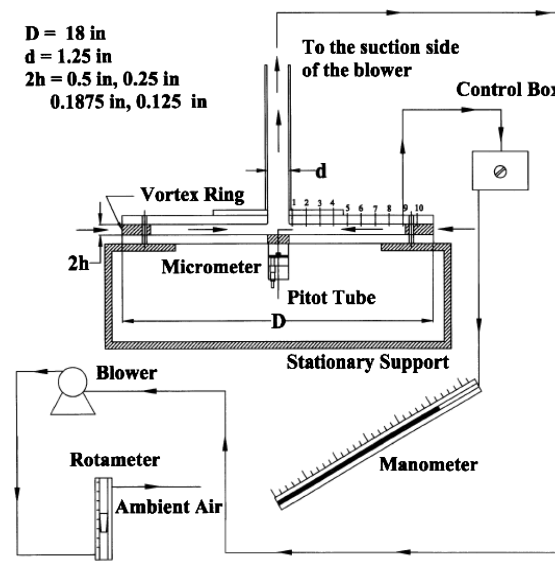

Fig. 2 Experimental apparatus.

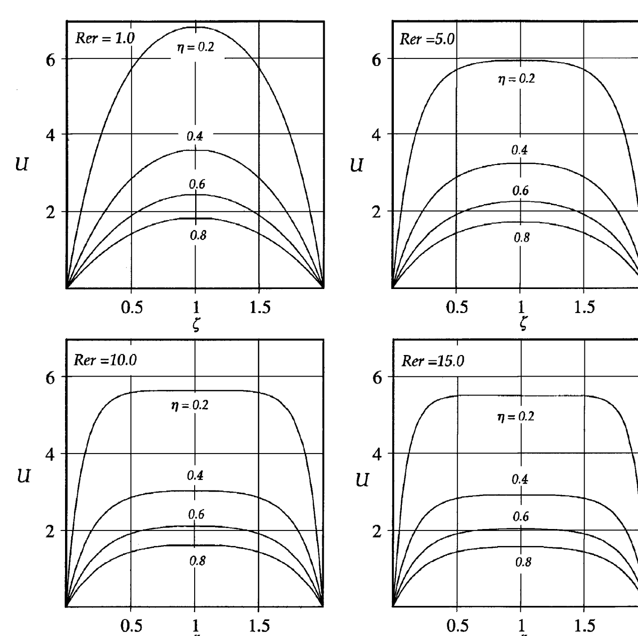

Fig. 3 Theoretical profiles of the radial-velocity at different radii as a function of Reynolds number Re_r.

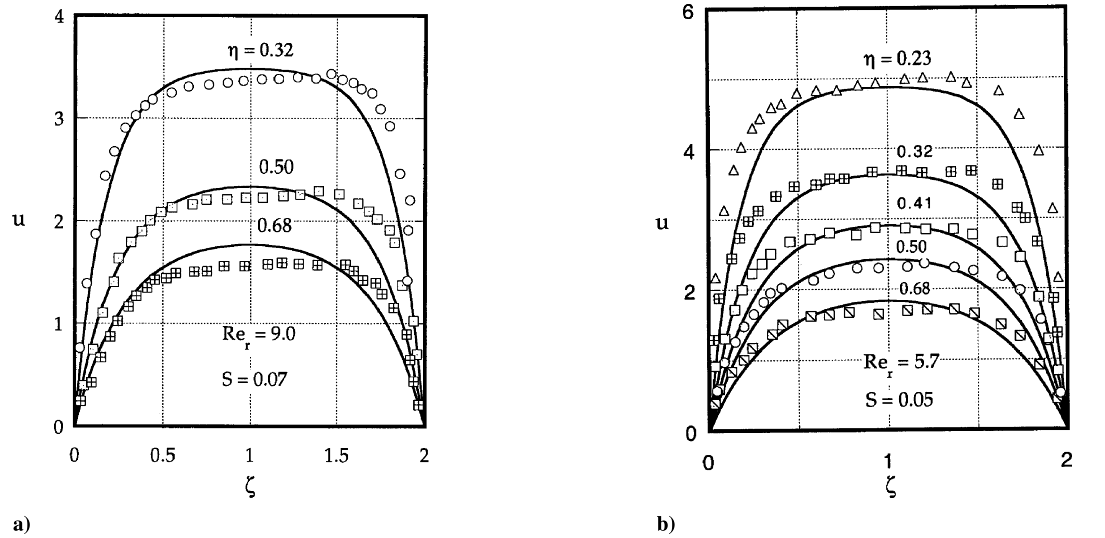

Fig. 4 Comparisons of the radial velocity distributions from present theory, and experiments of DeSantis and Rakowsky.[16]

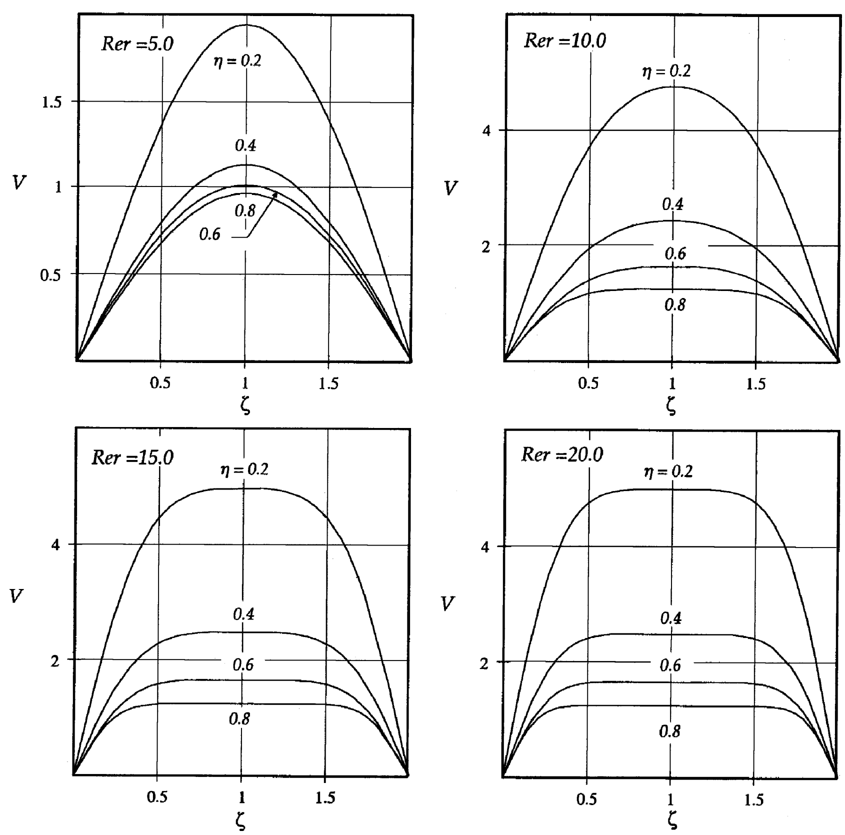

Fig. 5 Theoretical profiles of the tangential velocity at different radii as function of Reynolds number Re_r for stationary disks with swirl at inlet.

As Reynolds number Re_r increases, the velocity profile flattens midgap ($\zeta = 1$). The plateau progressively expands toward the walls ($\zeta = 0$ and $\zeta = 2$), where the velocity is seen to reduce to zero within a thin layer. Comparison with the experimental data of DeSantis and Rakowsky[16] is shown in Fig. 4. The radial velocity has been measured using a rotating hot wire. It is evident that there is a difficulty in resolving adequately the velocity near the walls. This is especially true in the neighborhood of the lower disk ($\zeta = 2$ in Fig. 4). Nevertheless, the data do provide some indication regarding the development of the radial velocity.

It would have been also interesting to confirm experimentally the theoretically obtained conjecture about the form of the latter velocity for stationary disks with swirl flow at the inlet. The only reliable experimental data for the radial velocity in such geometry are those of Savino and Keshock.[14] Unfortunately, these pertain to relatively large gaps ($h/R_{\text{in}} \approx 0.1$), a condition for the radial velocity that is outside the range of the present study. As the fluid enters the gap through the inlet, a strong centrifugal force field immediately confronts it. In its attempt to find the outlet with the least opposition, it does so by flowing closely to the disks where the tangential velocity reduces to satisfy the nonslip condition on the solid wall. The last produces the Ekman's boundary layers, which are characterized by two radial velocity peaks near the plates, thus, making them unsuitable for comparisons to the present asymptotic flow solution. For

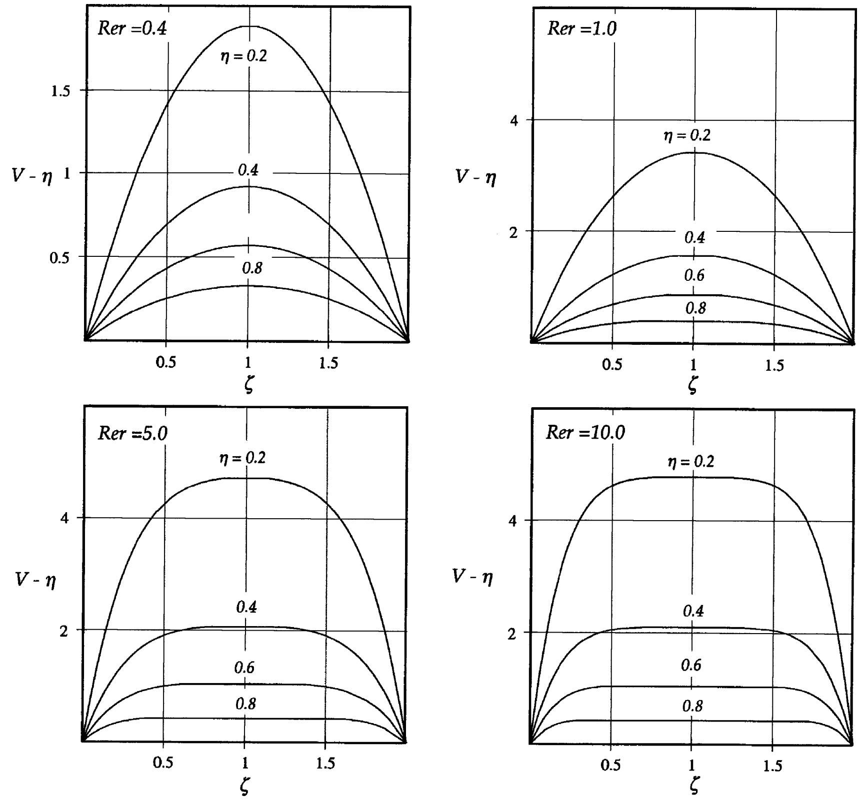

Fig. 6 Theoretical profiles of the tangential velocity at different radii as function of Reynolds number Re_r for corotating disks with swirl at inlet.

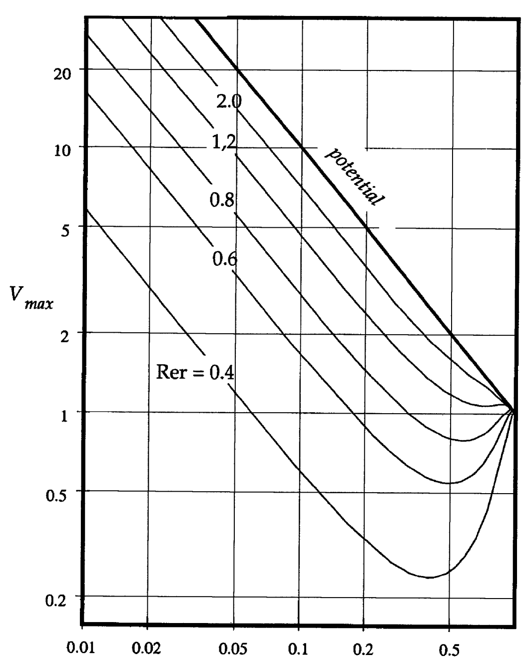

Fig. 7 Maximum tangential velocity as a function of η and Reynolds number Re_r for stationary disks with swirl at inlet.

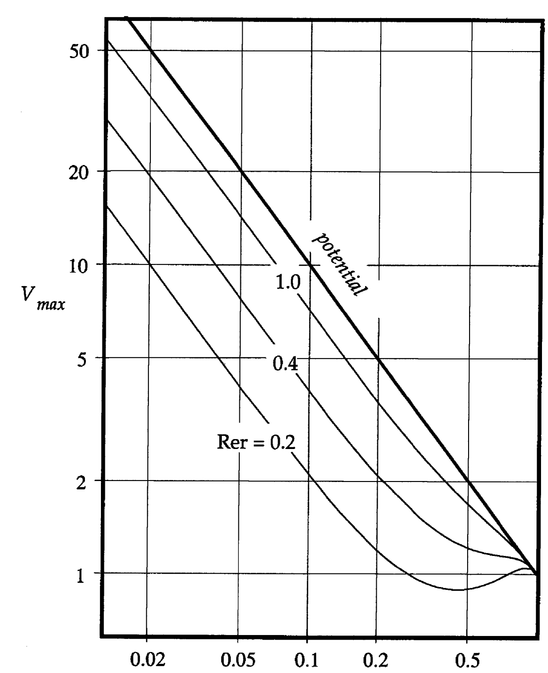

Fig. 8 Maximum tangential velocity as a function of η and Reynolds number Re_r for corotating disks with swirl at inlet.

considerably smaller gap ratios, the layers, however, are expected to merge and, thus, approach the conditions of the present analysis. Indications that this is the case are present in Fig. 4, where the radial velocity is seen to develop a small depression midchannel, which is the initial stage of the development of Ekman's boundary layer.

The development of the tangential velocity component for the case of stationary and rotating disks with swirl at the inlet are shown in Figs. 5 and 6, respectively. It is evident that the tangential velocity exhibits characteristics similar to that of the radial velocity. For small values of Reynolds number Re_r, the familiar Poiseuille like profile appears. When Reynolds number Re_r increases, the velocity profile flattens midgap, progressively spreading toward the walls. A closer look at the tangential momentum equation reveals that vorticity is carried by convection in the η direction, whereas in the ζ direction it is diffused by only the action of viscosity. For large Reynolds number Re_r values, the diffusion is confined within the layers near

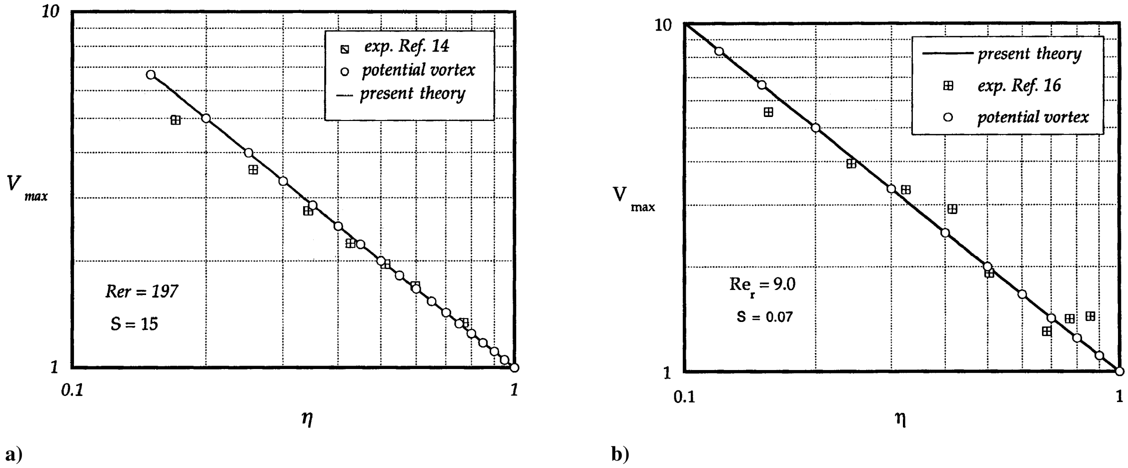

Fig. 9 Comparisons of the midgap tangential velocity from present theory and experiments of a) Savino and Keshock[14] and b) DeSantis and Rakowsky.[16]

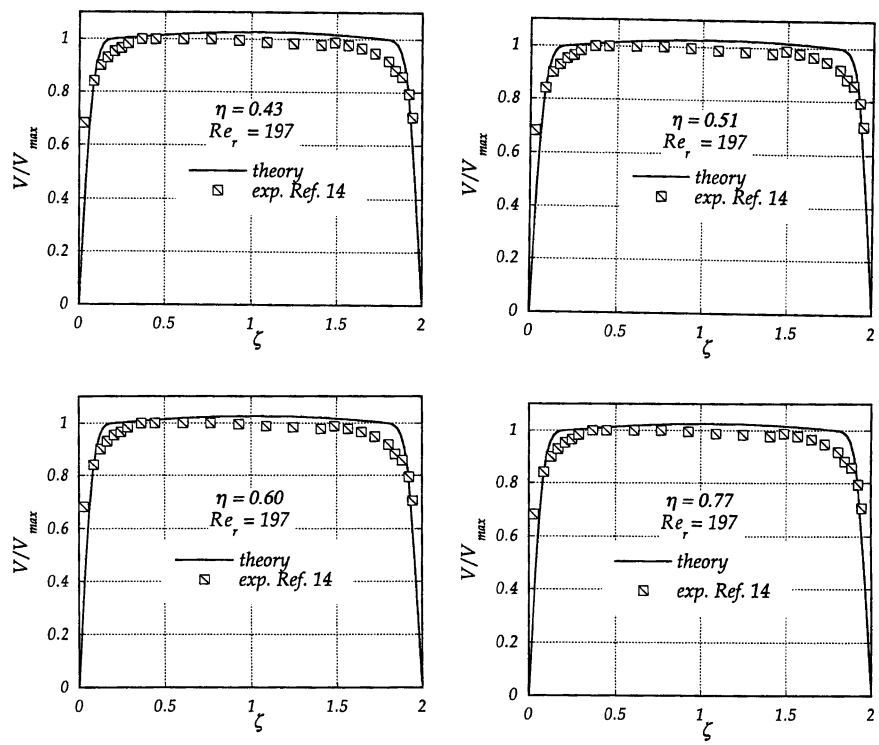

Fig. 10 Comparisons of the tangential velocity distributions from present theory and experiments of Savino and Keshock.[14]

the plates leaving the rest of the fluid in the ζ direction unaffected the action taking place near the solid walls.

The maximum tangential velocity occurs at the midchannel height, $\zeta = 1$. Its variation with the radius η is shown in Figs. 7 and 8. It is apparent that as Reynolds number Re_r increases both cases tend asymptotically to a potential vortex distribution. It is also evident that the rotating disk arrangement leads to the potential profile faster than the stationary disk case. In fact, for Re_r values of 12 and 9 for stationary and rotating disk situations, respectively, the maximum deviation from the free vortex is less than 0.1%. When $Re_r \to \infty$, the curvature of $V\eta \to 0$ at $\zeta = 1$; thus, from Eq. (10), $V_{\max}\,\eta \to 1$, which is the characteristic property of a potential vortex. For low Reynolds numbers, the maximum velocity first undergoes a decrease, gradually recovering afterward, tending to a power profile asymptotically for smaller radii. Therefore, for high Reynolds number Re_r values, as amply evident from the experiments of Savino and Keshock[14] (Fig. 9a) and DeSantis and Rakowsky[16] (Fig. 9b), the midgap value of the tangential velocity must be close to the free vortex. The value for $\eta = 0.15$ (Ref. 14) is the exemption; however, one has to realize that this point is inside the outlet tube ($R_e\,/\,R_{\text{in}} = 0.2$) where the flow is turning toward the exit. In fact, the diminishing deviations of points $\eta = 2.0$, 0.25, and 3.0 from the free vortex might also be due to the same effect. Comparisons between the experimental[14] and theoretical [Eq. (11)] tangential velocity distribution are found in Fig. 10. It is well known that in the case of strongly swirling flow, such as in the Savino and Keshock experiments, the tangential velocity dominates the other two components. It is, therefore, no surprise to find the theoretical tangential velocity to agree reasonably well with the experiment, whereas the radial velocity may not.

It has been shown previously that, in the case of relatively large Reynolds number Re_r values, the tangential velocity at the midplane tends to the free-vortex profile. Consequently,

$$\int_1^{\eta} \frac{V_{\max}^2}{\eta}\,\mathrm{d}\eta \to \frac{\eta^2 - 1}{2\eta^2}$$

or

$$\Delta\Pi(\lambda) = \Delta\Xi(\lambda) + S^2$$

For this particular condition, the pressure $\Delta\Pi$ is only a function of parameter λ. Profiles of the static pressure as a function of λ for different swirl ratios S are shown in Fig. 11. The majority of the experimental[9,14,18] points in Fig. 11 pertain to $S = 0$. Nevertheless, the pressure reported in Ref. 14 ($S \approx 15$) correlate reasonably well with the present theory.

For relatively small Reynolds number Re_r values, for example, $Re_r < 12$ for stationary disks and $Re_r < 9$ for rotating disks, the original pressure equation

$$\Delta p(\eta) = \Delta\Xi(\eta)\frac{\eta^2 - 1}{2\eta} + S^2 \int_1^\eta \frac{V_{\max}^2}{\eta}\,\mathrm{d}\eta$$

must be used. Confirmation of its validity is shown in Fig. 12.

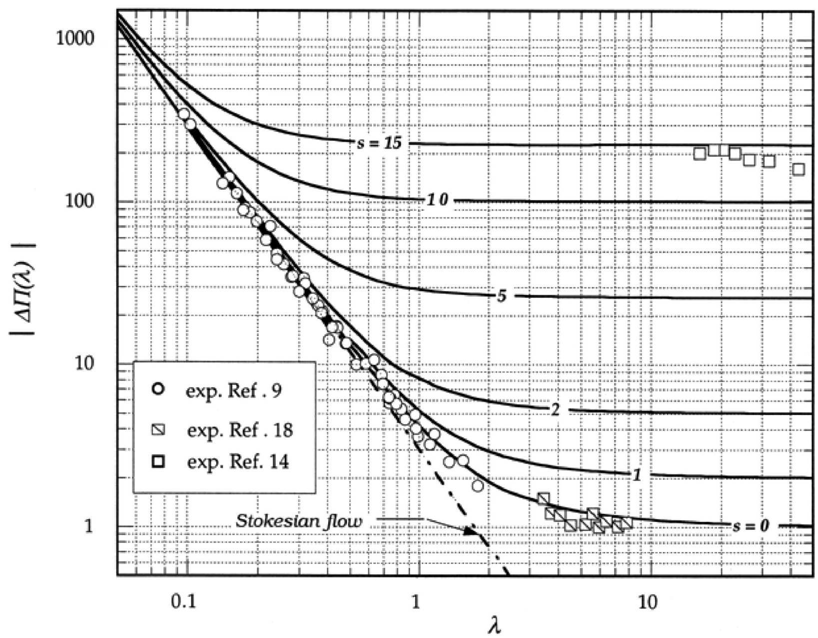

Fig. 11 Pressure variation with λ for different inlet swirl ratios, $Re_r > 12$ and 9 for stationary and corotating disks, respectively.

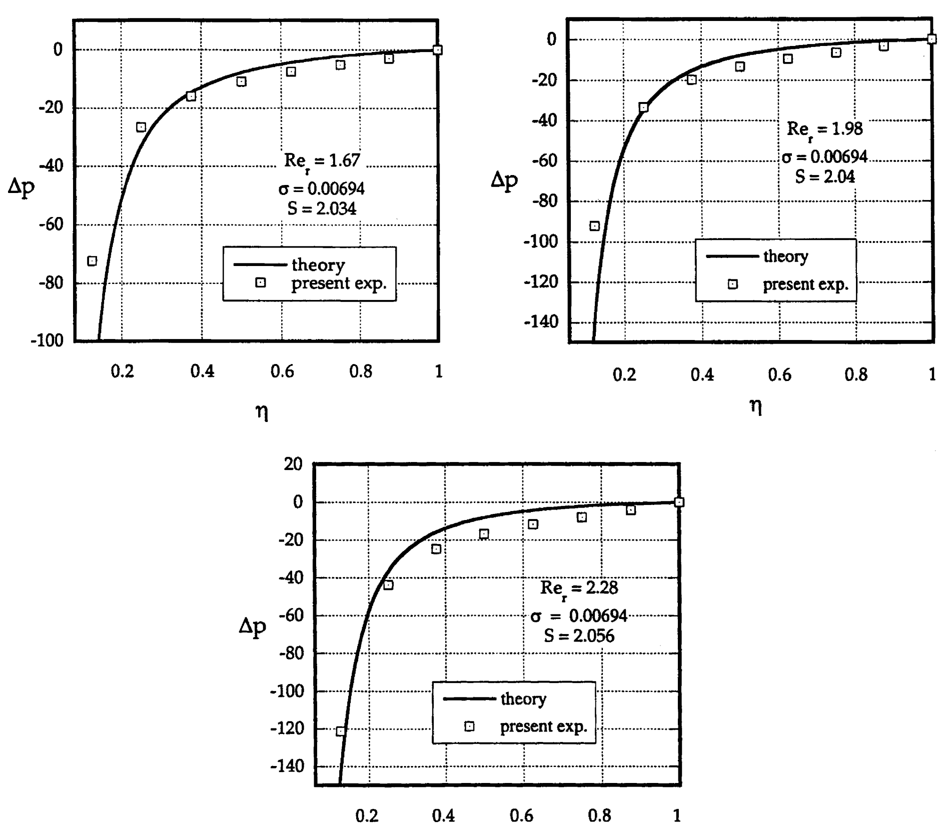

Fig. 12 Pressure variation with η for stationary disks with swirl at inlet, different inlet for $Re_r < 12$.

IV. Conclusions

We focused on asymptotic solutions to steady, laminar, swirling sink flow between two flat disks, where all material elements are monotonically accelerating in the radial direction. Although in the present problem the spacing between the two disks remain constant, the flowfield experiences a continuous acceleration because the area normal to the fluid motion changes with the radius. The analysis has shown the radial velocity component to depend solely on a single parameter, which combines the reduced Reynolds number and radial position. For large Reynolds numbers, the latter velocity component flattens in the middle of the channel, thus, developing a plateau that progressively expanded toward the disks. The tangential velocity component exhibited a similar property. The static pressure has been shown to depend on the vortex strength and the Reynolds number, with the centerline value approaching the free-vortex profile asymptotically. The results of the present analytical study compares reasonably well with previous and present experimental evidence.

References

[1]Morgan, P. G., and Saunders, A., "An Experimental Investigation of Inertia Effects in Viscous Flow," *International Journal of Mechanical Sciences*, Vol. 2, No. 1/2, 1960, pp. 8–12.

[2]Woolard, H. W., "A Theoretical Analysis of Viscous Flow in Narrowly Spaced Radial Diffuser," *Journal of Applied Mechanics*, Vol. 24, No. 1, March 1957, pp. 9–15.

[3]Livesey, J. L., "Inertia Effects in Viscous Flows," *International Journal of Mechanical Sciences*, Vol. 1, No. 1, 1960, pp. 84–88.

[4]Moller, P. S., "Radial Flow Without Swirl Between Parallel Discs," *Aeronautical Quarterly*, Vol. 14, May 1963, pp. 163–185.

[5]Boyack, B. E., and Rice, W., "An integral for Laminar Radial Outflow of Viscous Fluid Between Parallel Stationary Disks," *Journal of Basic Engineering*, Trans ASME, Vol. 92, No. 3, Sept. 1970, pp. 662, 663.

[6]Kwok, C., and Lee, P. M., "Integral Equation Method for Compressible Flow Between Parallel Disks," *Transactions of the Canadian Society for Mechanical Engineering*, Vol. 5, No. 1, 1979, pp. 55–58.

[7]Savage, S. B., "Laminar Flow Between Parallel Plates," *Journal of Applied Mechanics*, 1964, pp. 594, 595.

[8]Lee, P. M., and Lin, S., "Pressure Distribution for Radial Inflow Between Narrowly Spaced Disks," *Journal of Fluids Engineering*, Vol. 107, No. 3, Sept. 1985, pp. 338–341.

[9]Hayes, W. F., and Tucker, H. G., "Theoretical Radial Pressure Distribution for Viscous Fluid Inflow Within a Thin Disk Chamber," Rept. NRC-CS-51, National Research Council of Canada, Ottawa, 1973.

[10]Vatistas, G. H., "Radial Flow Between Closely Placed Flat Disks," *AIAA Journal*, Vol. 26, No. 7, 1988, pp. 887–889.

[11]Vatistas, G. H., "Radial Flow Within Two Flat Disks," *AIAA Journal*, Vol. 28, No. 7, 1990, pp. 1308–1310.

[12]Murphy, H. D., Chambers, F. W., and McEligot, D. M., "Laterally Converging Flow. Part 1. Mean Flow," *Journal of Fluid Mechanics*, Vol. 127, 1983, pp. 379–401.

[13]Zitouni, G., and Vatistas, G. H. "Purely Accelerating and Decelerating Flows Within Two Flat Disks," *Acta Mechanica*, Vol. 123, No. 1–4, 1997, pp. 151–161.

[14]Savino, J. M., and Keshock, E. G., "Experimental Profiles of Velocity Components and Radial Pressure Distributions in a Vortex Contained in a Short Cylindrical Chamber," NASA TN D-3072, Oct. 1965.

[15]Conover, R. A., "Laminar Flow Between a Rotating Disk and a Parallel Stationary Wall with and Without Radial Flow," *Journal of Basic Engineering*, Vol. 90, Sept. 1968, pp. 325–332.

[16]DeSantis, M. J., and Rakowsky, E. L., "An Experimental Investigation of the Viscous Flow Field in a Pneumatic Vortex Rate Sensor," *The American Society of Mechanical Engineers Fluidics Conference*, The American Society of Mechanical Engineers, Paper No. 70-Flcs-16, Atlanta, June 1970.

[17]Bakke, E., Kreider, J. F., and Kreith, F., "Turbulent Source Flow Between Parallel Stationary and Co-Rotating Disks," *Journal of Fluid Mechanics*, Vol. 58, Pt. 2, 1973, pp. 209–231.

[18]Singh, A., "Theoretical and Experimental Investigations on Inward Flow Between Two Disks," Ph.D. Dissertation, Dept. of Mechanical Engineering, Indian Inst. of Technology Bombay, Bombay, India 1993.